

# Rapid variations of mesophyll conductance in response to changes in CO<sub>2</sub> concentration around leaves

JAUME FLEXAS<sup>1</sup>, ANTONIO DIAZ-ESPEJO<sup>2</sup>, JERONI GALMÉS<sup>1</sup>, RALF KALDENHOFF<sup>3</sup>, HIPÓLITO MEDRANO<sup>1</sup> & MIQUEL RIBAS-CARBO<sup>1</sup>

<sup>1</sup>Grup de Recerca en Biologia de les Plantes en Condicions Mediterrànies, Departament de Biologia, Universitat de les Illes Balears. Carretera de Valldemossa Km 7.5, 07122 Palma de Mallorca, Balears, <sup>2</sup>Instituto de Recursos Naturales y Agrobiología, CSIC & Apartado 105241080 Sevilla, Spain and <sup>3</sup>Darmstadt University of Technology, Institute of Botany, Applied Plant Sciences, Schnittpahnstrasse 10, D-64287 Darmstadt, Germany

## ABSTRACT

The effects of short-term (minutes) variations of CO<sub>2</sub> concentration on mesophyll conductance to CO<sub>2</sub> ( $g_m$ ) were evaluated in six different C<sub>3</sub> species by simultaneous measurements of gas exchange, chlorophyll fluorescence, online carbon isotope discrimination and a novel curve-fitting method. Depending on the species,  $g_m$  varied from five- to ninefold, along the range of sub-stomatal CO<sub>2</sub> concentrations typically used in photosynthesis CO<sub>2</sub>-response curves ( $A_N$ - $C_i$  curves; where  $A_N$  is the net photosynthetic flux and  $C_i$  is the CO<sub>2</sub> concentrations in the sub-stomatal cavity), that is, 50 to 1500  $\mu\text{mol CO}_2 \text{ mol}^{-1}$  air. Although the pattern was species-dependent,  $g_m$  strongly declined at high  $C_i$ , where photosynthesis was not limited by CO<sub>2</sub>, but by regeneration of ribulose-1,5-bisphosphate or triose phosphate utilization. Moreover, these changes on  $g_m$  were found to be totally independent of the velocity and direction of the  $C_i$  changes. The response of  $g_m$  to  $C_i$  resembled that of stomatal conductance ( $g_s$ ), but kinetic experiments suggested that the response of  $g_m$  was actually faster than that of  $g_s$ . Transgenic tobacco plants differing in the amounts of aquaporin NtAQP1 showed different slopes of the  $g_m$ - $C_i$  response, suggesting a possible role for aquaporins in mediating CO<sub>2</sub> responsiveness of  $g_m$ . The importance of these findings is discussed in terms of their effects on parameterization of  $A_N$ - $C_i$  curves.

**Key-words:**  $A_N$ - $C_i$  curves; aquaporins; photosynthesis; leaf internal conductance.

## INTRODUCTION

Photosynthesis requires diffusion of CO<sub>2</sub> from the atmosphere into the leaf and finally to the site of carboxylation in the chloroplast stroma. From Fick's first law of diffusion, the net photosynthetic flux ( $A_N$ ) can be expressed as  $A_N = g_s(C_a - C_i) = g_m(C_i - C_c)$ ; where  $C_a$ ,  $C_i$  and  $C_c$  are the CO<sub>2</sub> concentrations ( $\mu\text{mol mol}^{-1}$  air) in the atmosphere, the sub-stomatal cavity and the chloroplast stroma,

Correspondence: J. Flexas. Fax: 34-971-173184; e-mail: jaume.flexas@uib.es

respectively, with  $g_s$  and  $g_m$  being the stomata and mesophyll conductances, respectively (Long & Bernacchi 2003).

Gas-exchange studies usually assumed that  $g_m$  was large and constant, that is, that  $C_i \approx C_c$  (Farquhar, von Caemmerer & Berry 1980). However, there is now evidence that  $g_m$  may be sufficiently small as to significantly decrease  $C_c$  relative to  $C_i$ , therefore limiting photosynthesis (Evans *et al.* 1986; Di Marco *et al.* 1990; Harley *et al.* 1992; Loreto *et al.* 1992; Warren 2006). Moreover,  $g_m$  is not constant, and it has been shown to acclimate during leaf development (Miyazawa & Terashima 2001) and senescence (Loreto *et al.* 1994; Grassi & Magnani 2005), as well as to the prevailing light (Hanba, Kogami & Terashima 2002; Niinemets *et al.* 2006), nutrient (Warren 2004) and watering conditions (Galmés, Medrano & Flexas 2006) during growth. There is also evidence of rapid variation of  $g_m$  in response to leaf temperature (Bernacchi *et al.* 2002; Warren & Dreyer 2006), water stress (Flexas *et al.* 2002, 2004; Grassi & Magnani 2005), salinity (Bongi & Loreto 1989; Loreto, Centritto & Chartzoulakis 2003) and virus infections (Sampol *et al.* 2003). Recently, substantial evidence has been compiled suggesting a role of aquaporins in the regulation of  $g_m$  (Hanba *et al.* 2004; Flexas *et al.* 2006). Aquaporin activity can be regulated by different mechanisms, including direct phosphorylation of aquaporins (Kjellbom *et al.* 1999), an osmotically driven cohesion/tension mechanism (Ye, Wiera & Steudle 2004), pH-dependent gating of aquaporins (Tournaire-Roux *et al.* 2003), and transcriptional regulation and protein stability (Eckert *et al.* 1999), most of them operating in short times (seconds to hours). Therefore, as already shown for temperature (Bernacchi *et al.* 2002; Warren & Dreyer 2006), it is likely that rapid variations in  $g_m$  can be induced by transient changes in the most common environmental conditions, including light intensity, relative humidity, wind speed or CO<sub>2</sub> concentration.

Regarding CO<sub>2</sub> concentration, in their early formulation of the two most common fluorescence methods used to estimate  $g_m$ , Harley *et al.* (1992) explicitly stated that 'The constant J method worked well over a large range of CO<sub>2</sub>, but to resolve the effect of CO<sub>2</sub> on  $g_m$  required the variable J method'. However, despite its evident interest to understand plant responses to climate change as well as for the

correct interpretation of  $A_N-C_i$  curves, the response of  $g_m$  to varying CO<sub>2</sub> has received only little attention over the past 15 years. The original data by Harley *et al.* (1992) showed that  $g_m$  was almost halved when  $C_i$  was increased from 100 to 300  $\mu\text{bar}$  in *Quercus rubra*, but not in *Eucalyptus globulus*. Moreover, using the isotopic method, Loreto *et al.* (1992) demonstrated that  $g_m$  was reduced at 750 mbar  $C_i$  as compared to ambient CO<sub>2</sub> in *Q. rubra* and, specially, in *Xanthium strumarium*. Surprisingly, these authors did not discuss the implications of these apparent variations of  $g_m$  at different CO<sub>2</sub> concentrations (Harley *et al.* 1992; Loreto *et al.* 1992). More than 10 years later, Düring (2003) was the first to show in grapevines that the  $g_m$  estimated using the variable fluorescence method varied as much as sixfold in a range of CO<sub>2</sub> from 50 to 2000  $\mu\text{mol mol}^{-1}$  air during the performance of a typical  $A_N-C_i$  curve (i.e. within minutes). On the other hand, Centritto, Loreto & Chartzoulakis (2003) showed in salt-stressed olives that, after maintaining the leaves for an hour at very low CO<sub>2</sub>, they recovered an  $A_N-C_i$  curve similar to control leaves. The effect could not be explained by the increased stomatal conductance only, but also required a concomitant increase in mesophyll conductance. It was therefore concluded that the response of  $g_m$  might be as rapid and reversible as that of  $g_s$  (Centritto *et al.* 2003). Flexas *et al.* (2004) showed a similar effect in drought-stressed sunflower. Regarding long-term acclimation to high CO<sub>2</sub>,  $g_m$  has been observed to decrease only in one species, but not in others (Singsaas, Ort & De Lucia 2004; Bernacchi *et al.* 2005). Finally, using a novel  $A_N-C_i$  curve-fitting method to estimate  $g_m$ , the values obtained were reported to depend somewhat on the number and range of the specific points considered along the curve (Ethier *et al.* 2006), although these authors attributed it to a mathematical artefact rather than to changes in  $g_m$  along the curve.

Despite all this evidence, the possible effects of CO<sub>2</sub> on the regulation of  $g_m$  are not usually taken into account. Actually, at least three commonly used methods for estimating  $g_m$ , that is, the constant J method (Harley *et al.* 1992), the slope-based variable fluorescence method (Terashima & Ono 2002) and the  $A_N-C_i$  curve-fitting method (Ethier & Livingston 2004; Ethier *et al.* 2006), rely on the assumption that  $g_m$  is not affected by CO<sub>2</sub> concentration. On the other hand, it is now recognized that a proper analysis using the Farquhar *et al.* (1980) model of photosynthesis must be done on a  $C_c$  rather than on a  $C_i$  basis (Long & Bernacchi 2003). However, most of the studies transform  $A_N-C_i$  curves to  $A_N-C_c$  curves using a single value of  $g_m$  determined at ambient CO<sub>2</sub> concentration, that is, also neglecting the possible effects of CO<sub>2</sub> on  $g_m$  (Flexas *et al.* 2002; Manter & Kerrigan 2004; Grassi & Magnani 2005).

Therefore, the objectives of the present work were (1) to characterize variations of  $g_m$  in response to rapid (minutes) changes in CO<sub>2</sub> concentration in different species, (2) to validate the results using independent methods for the estimation of  $g_m$  and (3) to discuss how these variations would affect the use of different methods to estimate  $g_m$  and the

correct analysis and interpretation of the most commonly used photosynthesis model (Farquhar *et al.* 1980), which is based on the response of net photosynthesis to CO<sub>2</sub> concentration at the site of ribulose-1,5-bisphosphate carboxylase/oxygenase (Rubisco).

## MATERIAL AND METHODS

### Plant material and growing conditions

Three-year-old olive trees (*Olea europaea* var. *europaea*) and 2-year-old plants of Richter-110 (a hybrid of *Vitis berlandieri*  $\times$  *Vitis rupestris*) were growing outdoors under typical Mediterranean conditions in the experimental field of the University of the Balearic Islands. Olive trees were rooted in a clay-calcareous soil, while *Vitis* plants were growing in 40 L pots containing a mixture of perlite, horticultural substrate and clay. The measurements in olives were made during winter (early March), while in *Vitis* were made during summer (early August). The other species, including cucumber (*Cucumis sativus* L.), arabidopsis [*Arabidopsis thaliana* (L.) Heyhn. genotype Col-0], tobacco (*Nicotiana tabacum* L. var. Samsun), flowering tobacco (*Nicotiana sylvestris* L.) and *Limonium gibertii* (Sennen) Sennen were grown in a growth chamber in 10 L pots containing a mixture of perlite, horticultural substrate and clay. Transformed tobacco (*N. tabacum* L.) plants with different levels of aquaporin NtAQP1, differing in mesophyll conductance to CO<sub>2</sub> (Flexas *et al.* 2006), were also studied. Antisense and overexpressing plants were obtained from different lines: var. Samsun for the antisense (AS) lines (Siefritz *et al.* 2002) and line Hö 20.20 for the overexpressing (O) lines (Uehlein *et al.* 2003). Plants of each line with normal NtAQP1 expression were used as controls (CAS and CO). The environmental conditions were set to a 12 h photoperiod (25 °C day/20 °C night), 40–60% relative humidity and a photon flux density at plant height of ca. 900  $\mu\text{mol m}^{-2} \text{s}^{-1}$  (halogen lamps), except in *Arabidopsis* (300  $\mu\text{mol m}^{-2} \text{s}^{-1}$ ). All plants were daily irrigated at field capacity.

### Gas-exchange and chlorophyll fluorescence measurements

All measurements were made on young, fully expanded leaves. Respiration in the light or 'day' respiration ( $R_d$ ) and the apparent CO<sub>2</sub> photocompensation point ( $C_i^*$ ) were determined according to the method of Laisk (1977) as described in von Caemmerer (2000).  $A_N-C_i$  curves were measured, using an open gas-exchange system Li-6400 (Li-Cor Inc., Lincoln, NE, USA), at three different photosynthetically active photon flux densities (PPFDs) (50, 200 and 500  $\mu\text{mol m}^{-2} \text{s}^{-1}$ ) at six different CO<sub>2</sub> levels ranging from 300 to 50  $\mu\text{mol CO}_2 \text{ mol}^{-1}$  air. The intersection point of the three  $A_N-C_i$  curves was used to determine  $C_i^*$  (x-axis) and  $R_d$  (y-axis).  $C_i^*$  was used as a proxy for the chloroplastic CO<sub>2</sub> photocompensation point ( $\Gamma^*$ ), according to Warren & Dreyer (2006). These values ranged from 33  $\mu\text{mol CO}_2 \text{ mol}^{-1}$  air in *Olea* to 44  $\mu\text{mol CO}_2 \text{ mol}^{-1}$  air in

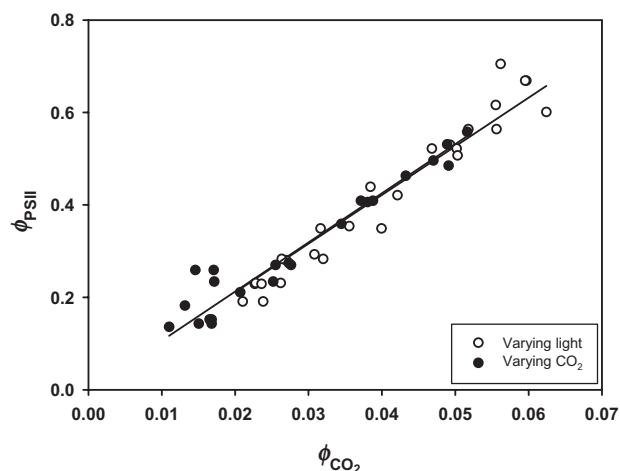


**Figure 1.** Example of the relationship between photochemical efficiency of photosystem II ( $\phi_{\text{PSII}}$ ) and  $\phi_{\text{CO}_2}$   $[(A_n + R_d)/\text{PPFD}]$  in tobacco leaves, obtained by varying either light intensity (empty symbols) or  $\text{CO}_2$  concentration (filled symbols) under non-photorespiratory conditions in an atmosphere containing less than 1%  $\text{O}_2$  (Valentini *et al.* 1995).

*Arabidopsis*, corresponding to Rubisco specificity factors between 85 and 112, that is, in good agreement with the reported values for  $\text{C}_3$  plants (Galmés *et al.* 2005).

All other leaf gas-exchange parameters were determined simultaneously with measurements of chlorophyll fluorescence using the open gas-exchange system Li-6400 (Li-Cor Inc.) with an integrated fluorescence chamber head (Li-6400-40; Li-Cor Inc.). The actual photochemical efficiency of photosystem II ( $\phi_{\text{PSII}}$ ) was determined by measuring steady-state fluorescence ( $F_s$ ) and maximum fluorescence during a light-saturating pulse of ca.  $8000 \mu\text{mol m}^{-2} \text{s}^{-1}$  ( $F_m'$ ) following the procedures of Genty, Briantais & Baker (1989):

$$\phi_{\text{PSII}} = (F_m' - F_s)/F_m' \quad (1)$$

The electron transport rate ( $J_{\text{flu}}$ ) was then calculated as

$$J_{\text{flu}} = \phi_{\text{PSII}} \cdot \text{PPFD} \cdot \alpha \cdot \beta \quad (2)$$

where PPFD is the photosynthetically active photon flux density,  $\alpha$  is leaf absorptance and  $\beta$  reflects the partitioning of absorbed quanta between photosystems II and I (PSI and PSII).  $\alpha$  was measured using a spectroradiometer (HR2000CG-UV-NIR; Ocean Optics Inc., Dunedin, FL, USA) as described by Schultz (1996), using the light source from the Li-6400 and making the measurements inside a dark chamber. In addition, the product  $\alpha \cdot \beta$  was determined from the relationship between  $\phi_{\text{PSII}}$  and  $\phi_{\text{CO}_2}$  obtained by varying either light intensity or  $\text{CO}_2$  concentration under non-photorespiratory conditions in an atmosphere containing less than 1%  $\text{O}_2$  (Valentini *et al.* 1995). An example of such relationships is shown in Fig. 1 for tobacco. No differences were observed when light intensity or  $\text{CO}_2$  concentration was changed. Therefore, only changes in light intensity were used for the other species. The

resulting  $\alpha$ , as determined with the spectroradiometer, ranged between 0.88 (*Arabidopsis*) and 0.95 (*Limonium*), in agreement with other reports using the Li-6400 light source (Niinemets *et al.* 2005). The product  $\alpha \cdot \beta$ , as determined according to Valentini *et al.* (1995), ranged between 0.35 (*Vitis*) and 0.45 (*Arabidopsis*), depending on the species. The resulting value of light partitioning towards PSII ( $\beta$ ) ranged between 0.39 and 0.51, that is, well within the range of typically reported values (Laisk & Loreto 1996).

$\text{CO}_2$ -response curves were performed in light-adapted leaves of six different plants for each species. Except when specifically indicated, photosynthesis was induced with a PPFD of  $1500 \mu\text{mol m}^{-2} \text{s}^{-1}$  (previously performed light-response curves had shown this to be sufficient light to saturate photosynthesis in all the species analysed) and  $400 \mu\text{mol mol}^{-1}$   $\text{CO}_2$  surrounding the leaf ( $C_a$ ). The amount of blue light was set to 10–15% PPFD to maximize stomatal aperture. Leaf temperature was close to  $25^\circ\text{C}$ , and leaf-to-air vapour pressure deficit was kept between 1.2 and 1.8 kPa during all measurements. Once steady state was reached (usually 30 min after clamping the leaf), a  $\text{CO}_2$ -response curve was performed. Gas exchange and chlorophyll fluorescence were first measured at  $400 \mu\text{mol mol}^{-1}$ , then  $C_a$  was either increased stepwise until  $1800 \mu\text{mol mol}^{-1}$  or decreased stepwise until  $50 \mu\text{mol mol}^{-1}$ . Upon completion of measurements at high or low  $C_a$ , this was returned to  $400 \mu\text{mol mol}^{-1}$  to restore the original  $A_n$ . Then,  $C_a$  was either decreased or increased (depending on the previous treatment) stepwise to complete the curve. The number of different  $C_a$  values used for the curves ranged between 10 and 12, depending on the species, and the time lag between two consecutive measurements at different  $C_a$  was restricted to 2–4 min, so that each curve was completed in 30–40 min.

Leakage of  $\text{CO}_2$  into and out the leaf cuvette was determined for the range of  $\text{CO}_2$  concentrations used in this study with photosynthetically inactive leaves of each species enclosed in the leaf chamber (obtained by heating the leaves until no variable chlorophyll fluorescence was observed), and used to correct measured leaf fluxes (Flexas *et al.* 2007).

### Estimation of $g_m$ by gas exchange and chlorophyll fluorescence

The method by Harley *et al.* (1992) was used to make estimations of  $g_m$  as

$$g_m = A_n / (C_i - (\Gamma^* \cdot (J_{\text{flu}} + 8 \cdot (A_n + R_d))) / (J_{\text{flu}} - 4 \cdot (A_n + R_d))) \quad (3)$$

where  $A_n$  and  $C_i$  are taken from gas-exchange measurements at saturating light and  $\Gamma^*$  and  $R_d$  were estimated using the Laisk (1977) method (see previous section).

The calculated values of  $g_m$  were used to convert  $A_n$ – $C_i$  curves into  $A_n$ – $C_c$  curves using the following equation:

$$C_c = C_i - (A_n / g_m) \quad (4)$$

From  $A_N-C_c$  curves, the maximum carboxylation capacity ( $V_{c,max}$ ) and the maximum capacity for electron transport rate ( $J_{max}$ ) were calculated using the temperature dependence of kinetic parameters of Rubisco described on a  $C_c$  basis by Bernacchi *et al.* (2002), whereby net assimilation rate is given as

$$A = \min\{A_c, A_q\} - R_d \quad (5)$$

with

$$A_c = V_{c,max} \frac{C_c - \Gamma^*}{C_c + K_c[1 + (o_i/K_o)]} \quad (6)$$

$$A_q = \frac{J(C_c - \Gamma^*)}{4(C_c + 2\Gamma^*)} \quad (7)$$

where  $A_c$  and  $A_q$  represent photosynthesis limited by carboxylation and RuBP regeneration, respectively,  $K_c$  and  $K_o$  are the Rubisco Michaelis-Menten constants for carboxylation and oxygenation, respectively, and  $o_i$  is the leaf internal oxygen concentration (assumed equal to the external).

### Estimation of $g_m$ by a curve-fitting method

A new curve-fitting method (Ethier & Livingston 2004; Ethier *et al.* 2006) was used to estimate  $g_m$  in some experiments. In short, the method by Ethier & Livingston (2004) fits  $A-C_i$  curves with a non-rectangular hyperbola version of the Farquhar's biochemical model of leaf photosynthesis. This is based on the hypothesis that  $g_m$  reduces the curvature of the  $A-C_i$  response curve. The combination of Eqn 4 with Eqns 6 and 7 yields the following quadratic equations, whose solutions are the positive roots:

$$A_c = \frac{-b + \sqrt{b^2 - 4ac}}{2a} \quad (8)$$

where

$$a = -1/g_m$$

$$b = (V_{c,max} - R_d)/g_m + C_i + K_c(1 + O/K_o)$$

$$c = R_d(C_i + K_c(1 + O/K_o)) - V_{c,max}(C_i - \Gamma^*)$$

$$A_q = \frac{-b + \sqrt{b^2 - 4ac}}{2a} \quad (9)$$

$$a = -1/g_m$$

$$b = (J/4 - R_d)/g_m + C_i + 2\Gamma^*$$

$$c = R_d(C_i + 2\Gamma^*) - J/4(C_i - \Gamma^*)$$

Values of  $K_c$ ,  $K_o$ ,  $\Gamma^*$  and their temperature responses, were the  $C_c$ -based *in vivo* values from Bernacchi *et al.* (2002). The

$C_i$  cut-off point was determined based on the method proposed by Ethier *et al.* (2006). This method has been successfully used in several studies, showing good agreement with other independent estimates of  $g_m$  (Niinemets *et al.* 2006; Warren & Dreyer 2006). Although some of the curves showed a third region, with photosynthesis limited by triose-phosphate use (e.g. *Limonium* in Fig. 1), the curve-fitting method was not applied to that region, because its parameterization is not straightforward (von Caemmerer 2000) and, depending on the equations chosen, it leads to arbitrary estimations of  $g_m$  (data not shown).

### Estimation of $g_m$ by carbon isotope discrimination at near to ambient and high CO<sub>2</sub>

Instantaneous carbon isotope discrimination was measured as previously described (Flexas *et al.* 2006). Leaves were placed in the chamber of the Li-6400 at 400  $\mu\text{mol mol}^{-1}$ , a PPFD of 1500  $\mu\text{mol m}^{-2} \text{s}^{-1}$  and at 25 °C. Gas-exchange parameters were measured as described with the Li-6400 system under steady-state conditions for a minimum of 45 min.

Once gas-exchange measurements were performed, the air exiting the cuvette was collected as follows: maintaining the leaf in the cuvette under steady state by maintaining the same conditions of light, CO<sub>2</sub> concentration and temperature, the exhaust tube was disconnected of the match valve and connected through a series of Swagelock tube connectors to a magnesium perchlorate (water trap) tube and to a handmade 100 mL glass flask with Teflon stopcocks (Ribas-Carbo, Still & Berry 2002). Under steady-state conditions, the air passed through the desiccant and the open collecting bottle for 15 min at a flow above 150 mL min<sup>-1</sup>, ensuring 20 full turnovers of air inside the collecting bottle before the stopcocks were closed and the bottle removed. In order to collect a reference air, the same procedure was followed with the cuvette empty.

Carbon isotope composition was determined in an isotope ratio mass spectrometer (IRMS) (Thermo Delta XPlus, Bremen, Germany) under dual-inlet mode. CO<sub>2</sub> from the bottles (sample and reference) was first concentrated in a Precon loop under liquid nitrogen and then introduced in its corresponding fully expanded bellows. The bellows were then compressed to increase the signal for the  $m/z$  44 peak to a minimum of 1000 mV to maximize the signal/noise ratio. The dual-inlet IRMS compared the isotope ratio of the sample and reference CO<sub>2</sub> introduced in its bellows. Firstly, the system performs a peak centre on ( $m/z$  45), then it equilibrates the sample and reference signal for the  $m/z$  44 peak and then both isotope ratios are compared 25 times. The SD of the  $\delta^{13}\text{C}$  of the sample CO<sub>2</sub> with respect to the reference CO<sub>2</sub> was always below 0.03‰.

Carbon isotope discrimination was calculated as described by Evans *et al.* (1986), as

$$\Delta^{13}\text{C}_{\text{obs}} = \left[ \frac{\xi(\delta^{13}\text{C}_o - \delta^{13}\text{C}_e)}{1000 + \delta^{13}\text{C}_o - \xi(\delta^{13}\text{C}_o - \delta^{13}\text{C}_e)} \right] \quad (10)$$

where  $\xi = C_e/(C_e - C_o)$ , and  $C_e$  and  $C_o$  are the  $\text{CO}_2$  concentrations of the air entering and leaving the chamber, respectively. Because of the dual-inlet comparison method used, the value of  $\delta^{13}\text{C}_e$  was equal to 0 and  $\delta^{13}\text{C}_o$  was the value obtained from the isotope analysis.

Mesophyll conductance values were determined by comparing predicted discrimination with observed discrimination. Predicted discrimination ( $\Delta_i$ ) was calculated from the following equation by Evans *et al.* (1986):

$$\Delta_i = a + (b - a) p_i / p_a \quad (11)$$

where  $a$  is the fractionation occurring due to diffusion in air (4.4‰),  $b$  is the net fractionation by Rubisco and phosphoenolpyruvate carboxylase (PEPC) (29‰), and  $p_i$  and  $p_a$  are the intercellular and ambient partial pressures of  $\text{CO}_2$ , respectively.

Finally,  $g_m$  was calculated from the equation (Evans & von Caemmerer 1996):

$$\Delta_i - \Delta_{\text{obs}}^{13} = (29 - 1.8)(A_N / g_m) / p_a \quad (12)$$

where 1.8‰ is the discrimination due to dissolution and diffusion of  $\text{CO}_2$  in water.

After collecting air from the cuvette at  $400 \mu\text{mol CO}_2 \text{ mol}^{-1}$  air,  $C_a$  was increased to  $1500 \mu\text{mol CO}_2 \text{ mol}^{-1}$  air, and the leaf allowed acclimating for 15 min. Then, air collecting and  $g_m$  determinations were repeated as described.

## RESULTS

Fast  $A_N$ - $C_i$  curves (30 to 45 min) were analysed in up to six different  $\text{C}_3$  species (Fig. 2). The initial portion of the curve showed almost linear dependence of  $A_N$  versus  $C_i$ , indicating limitation by carboxylation. A second portion was clearly curvilinear, indicating limitation by regeneration of ribulose-1,5-bisphosphate. In three of the species (*Arabidopsis*, *Limonium* and *Vitis*), the curves displayed a third

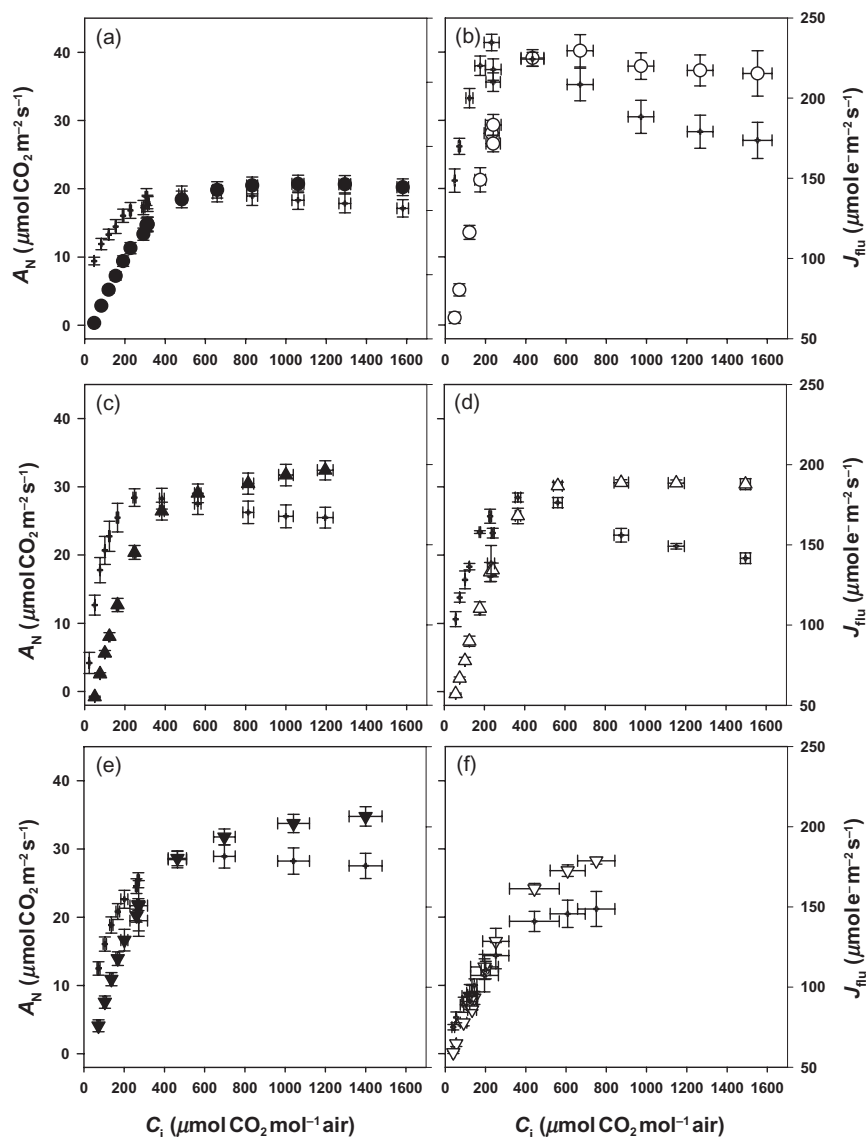


**Figure 2.** Response of net photosynthesis ( $A_N$ , large symbols) and electron transport rate ( $J_{\text{flu}}$ , crosshairs) to sub-stomatal  $\text{CO}_2$  concentrations ( $C_i$ ) in (a) *Arabidopsis thaliana* (filled circles), (b) *Limonium gibertii* (empty circles), (c) *Nicotiana tabacum* (filled upwards triangles), (d) *Vitis berlandieri*  $\times$  *Vitis rupestris* (empty upwards triangles), (e) *Cucumis sativus* (empty downwards triangles) and (f) *Olea europaea* var. *europaea* (open downwards triangles). Values are averages  $\pm$  SE of three to six replicates, depending on the species.

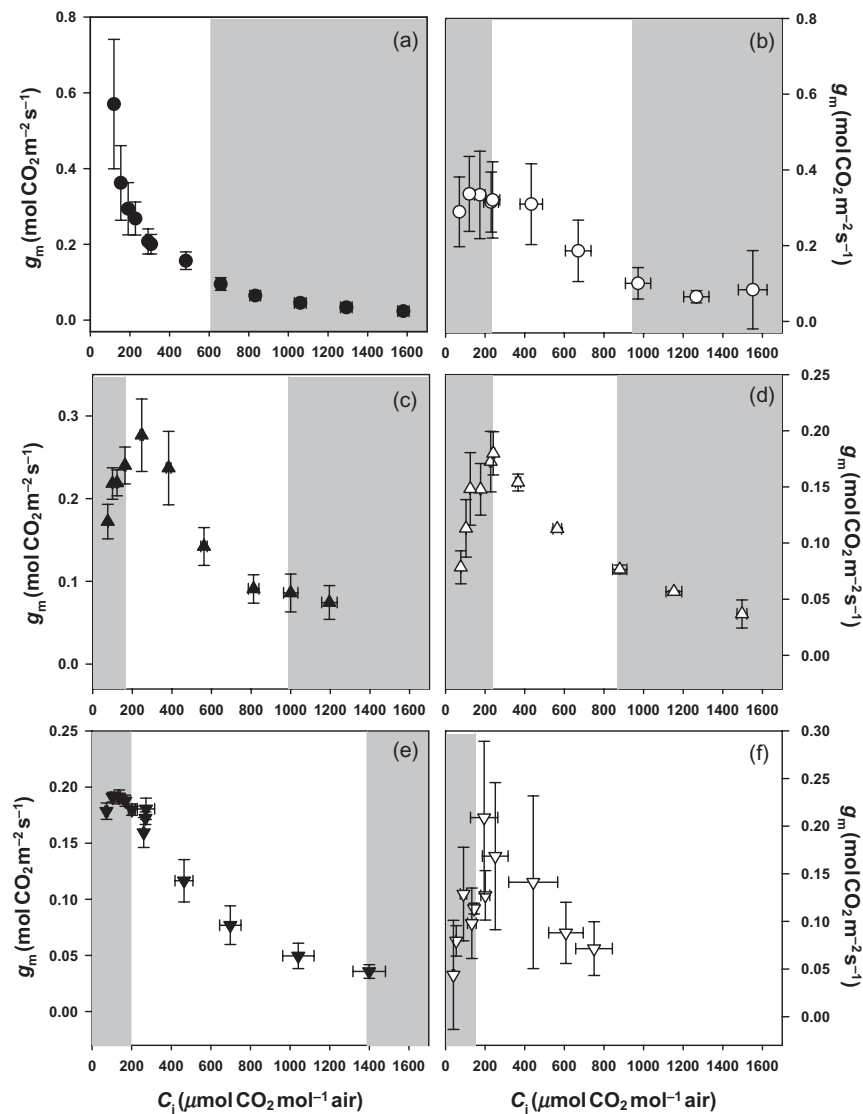


**Figure 3.** Response of mesophyll conductance ( $g_m$ ) to sub-stomatal  $\text{CO}_2$  concentrations ( $C_i$ ) in (a) *Arabidopsis thaliana* (filled circles), (b) *Limonium gibertii* (empty circles), (c) *Nicotiana tabacum* (filled upwards triangles), (d) *Vitis berlandieri* × *Vitis rupestris* (empty upwards triangles), (e) *Cucumis sativus* (empty downwards triangles) and (f) *Olea europaea* var. *europaea* (open downwards triangles). Values are averages  $\pm$  SE of three to six replicates, depending on the species. Un-shaded regions indicate  $g_m$  data with a  $dC_i/dA_N$  between 10 and 50, which are reliable according to Harley *et al.* (1992).

portion consisting of constant or slightly declining  $A_N$  with increasing  $C_i$ , indicating limitation by triose phosphate utilization.  $J_{\text{flu}}$  responded to  $C_i$  in a biphasic mode in all species except *Olea*, with maximum  $J_{\text{flu}}$  being at  $C_i$  between 200 and  $600 \mu\text{mol CO}_2 \text{ mol}^{-1} \text{ air}$ , depending on the species (Fig. 2). Such a biphasic response was already described by Sharkey, Berry & Sage (1988) under high light intensities, and it is thought to be due to feedback limitation by triose phosphate utilization. Because gas exchange was measured concomitantly with chlorophyll fluorescence, it was possible to estimate  $g_m$  for most  $C_i$  concentrations used, except at very low  $C_i$ , where  $A_N$  was close to zero or negative, resulting in strongly variable and often not reliable  $g_m$  estimates. At ambient  $\text{CO}_2$ ,  $g_m$  ranged from  $0.127 \text{ mol CO}_2 \text{ m}^{-2} \text{ s}^{-1}$  in *Olea* to  $0.315 \text{ mol CO}_2 \text{ m}^{-2} \text{ s}^{-1}$  in *Limonium*. If the bulk of the mesophyll resistance is in the liquid phase, it is theoretically more correct to include a pressure term in the units but for the purposes of this paper, we have used units without a pressure term for easier comparison between stomatal and

mesophyll conductance values. Atmospheric pressure during these measurements was close to 101 kPa.

Contrary to what was usually assumed,  $g_m$  was not constant along the range of  $C_i$  used for  $A_N$ - $C_i$  curves (Fig. 3). It has been suggested that the reliability of  $g_m$  data is questionable when  $dC_i/dA_N$  is lower than 10 or higher than 50 (Harley *et al.* 1992). These values are shown by shaded areas in Fig. 3 (left,  $dC_i/dA_N < 10$ ; right,  $> 50$ ). Taking into consideration the  $g_m$  values within the reliable range, it is observed that  $g_m$  decreases as  $C_i$  increases in all the species studied (Fig. 3). At high  $C_i$ ,  $g_m$  values are as low as 5 to 30% those at lower  $C_i$ .

Transgenic tobacco plants differing in the expression of aquaporin NtAQP1 and  $g_m$  (Flexas *et al.* 2006) also showed a similar dependence of  $g_m$  on  $C_i$  (Fig. 4). In these plants, the higher the  $g_m$  at ambient  $\text{CO}_2$ , the stronger its dependency on  $C_i$  was. Consequently, the largest differences between genotypes were observed at low  $C_i$  and vice versa (Fig. 4).

Several tests were performed in *Nicotiana* to demonstrate the independence of this pattern on the experimental

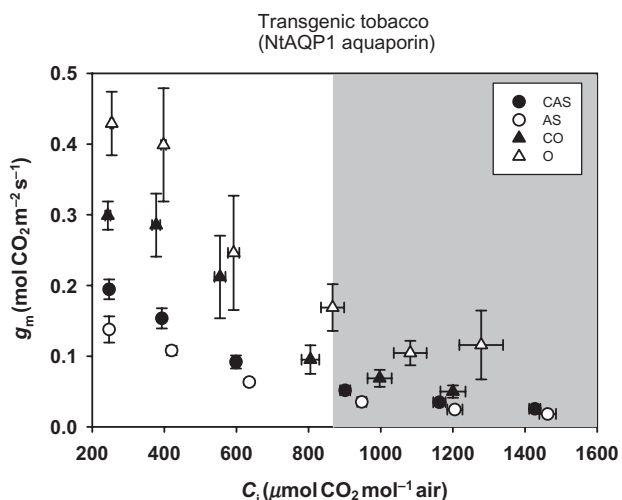


**Figure 4.** Response of mesophyll conductance ( $g_m$ ) to sub-stomatal  $\text{CO}_2$  concentrations ( $C_i$ ) in transgenic *Nicotiana* plants overexpressing aquaporin NtAQP1 (O, empty triangles) or anti-sense (AS, empty circles) and their respective wild-type lines (CO, filled triangles, and CAS, empty triangles). Only the declining portion of the  $g_m$ - $C_i$  relationship is shown for clarity. Values are averages  $\pm$  SE of six replicates. Un-shaded regions indicate  $g_m$  data with a  $dC_i/dA_N$  between 10 and 50, which are reliable according to Harley *et al.* (1992).

procedure. Firstly, the direction of changes in  $C_a$  was analysed. Therefore, curves performed by initially decreasing  $C_a$  from  $400 \mu\text{mol CO}_2 \text{ mol}^{-1}$  air to  $50 \mu\text{mol CO}_2 \text{ mol}^{-1}$  air, and then returned to  $400 \mu\text{mol CO}_2 \text{ mol}^{-1}$  air and increased to  $1800 \mu\text{mol CO}_2 \text{ mol}^{-1}$  air were compared to curves that were performed the opposite way. Curves of  $A_N$ ,  $J_{\text{flu}}$  and  $g_m$  versus  $C_i$  were almost identical (data not shown).

The interference of light intensity to  $g_m$  was also tested with several  $A_N$ - $C_i$  curves performed at lower light intensities (1000, 750 and  $250 \mu\text{mol m}^{-2} \text{ s}^{-1}$ ). Light intensity seemed to have some effect, because the dependency of  $g_m$  on  $C_i$  was larger at higher light intensity (Fig. 5). Nevertheless,  $g_m$  declined with increasing  $C_i$  in all cases. Finally, any possible effect that the short time employed between two consecutive measurements at different  $C_i$  could produce on  $g_m$  was tested. Different leaves were acclimated to different  $C_a$  until steady state of both  $A_N$  and  $g_s$  was reached (typically 45 to 60 min after clamping the leaf). Data from different leaves at different  $C_a$  were plotted together to produce an 'artificial'  $A_N$ - $C_i$  curve. The resulting plot was very similar to that of the 'real'  $A_N$ - $C_i$  curves shown in Fig. 3 (data not shown).

Therefore, it seems that, regardless of the procedure and conditions to modify  $C_i$ ,  $g_m$  showed a dependency of  $C_i$  similar to that of  $g_s$ . The velocity of response of both conductances was tested in *Nicotiana* (Fig. 6). Firstly,  $A_N$ ,  $J_{\text{flu}}$ ,  $C_i$ ,  $g_s$  and  $g_m$  were measured in steady state at almost ambient  $\text{CO}_2$ , then  $C_a$  was suddenly increased to  $1500 \mu\text{mol CO}_2 \text{ mol}^{-1}$  air, and the leaves allowed to acclimate to the new conditions for about 1 h.  $A_N$ ,  $J_{\text{flu}}$ ,  $C_i$ ,  $g_s$  and  $g_m$  were then determined. Finally,  $C_a$  was returned to  $400 \mu\text{mol CO}_2 \text{ mol}^{-1}$  air to follow  $g_s$  and  $g_m$  recovery (Fig. 6). Both  $g_s$  and  $g_m$  decreased at high  $\text{CO}_2$ .

Then, when  $C_a$  was returned to lower values, both conductances recovered progressively to their initial values.  $g_m$  almost fully recovered in about 15 min, while  $g_s$  needed about 45 min to fully recover.

The concomitant decrease of both  $g_s$  and  $g_m$  in response to increasing  $\text{CO}_2$  strongly reduced the chloroplast  $\text{CO}_2$  concentration ( $C_c$ ) with respect to ambient ( $C_a$ ), particularly at high  $\text{CO}_2$  concentrations. Overall, the  $C_i/C_a$  ratio ranged between 0.50 and 0.76 at  $400 \mu\text{mol CO}_2 \text{ mol}^{-1}$  air and, in most species, increased at  $1800 \mu\text{mol CO}_2 \text{ mol}^{-1}$  air (data not shown). By contrast, the  $C_c/C_a$  ratio ranged only between 0.25 and 0.57 at  $400 \mu\text{mol CO}_2 \text{ mol}^{-1}$  air and usually decreased at  $1800 \mu\text{mol CO}_2 \text{ mol}^{-1}$  air (data not shown).

To discard any possible artefact inherent to the fluorescence method, two totally independent methods were used to prove the effect of  $C_i$  on  $g_m$ . One experimental comparison was performed in leaves of *N. tabacum* to determine  $g_m$  by online carbon isotope discrimination (Evans *et al.* 1986) at two different  $\text{CO}_2$  concentrations, 400 and  $1500 \mu\text{mol CO}_2 \text{ mol}^{-1}$  air (Table 1). During this experiment, a second Li-6400 with chlorophyll fluorescence chamber was attached to the same leaves to simultaneously determine  $g_m$  by the Harley *et al.* (1992) method. Carbon isotope discrimination and fluorescence measurements resulted in similar estimations of  $g_m$  and confirmed that, at high  $C_i$ ,  $g_m$  was substantially reduced. However, these results could be affected by differences in respiration and photorespiration at the two  $\text{CO}_2$  concentrations, because total carbon isotope discrimination is affected by discrimination during both processes (Ghashghaie *et al.* 2003). While the contribution of respiration may be relatively small and not very different between  $\text{CO}_2$  concentrations, the rate of photorespiration is strongly affected by  $\text{CO}_2$ , and hence its associated discrimination. Therefore, an additional experiment was performed

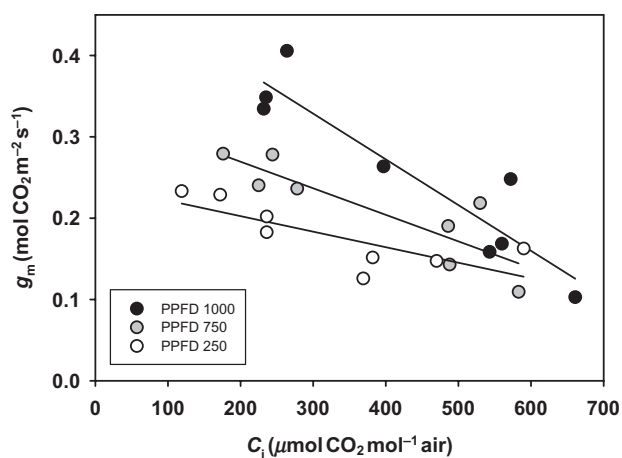


**Figure 5.** Response of mesophyll conductance ( $g_m$ ) to sub-stomatal  $\text{CO}_2$  concentrations ( $C_i$ ) in *Nicotiana* leaves illuminated at a photosynthetically active photon flux density (PPFD) of 1000 (black circles), 750 (grey circles) and 250 (white circles)  $\mu\text{mol m}^{-2} \text{ s}^{-1}$ . Only the data with a  $dC_i/dA_N$  between 10 and 50 are shown. The data shown are single curves for each light intensity.

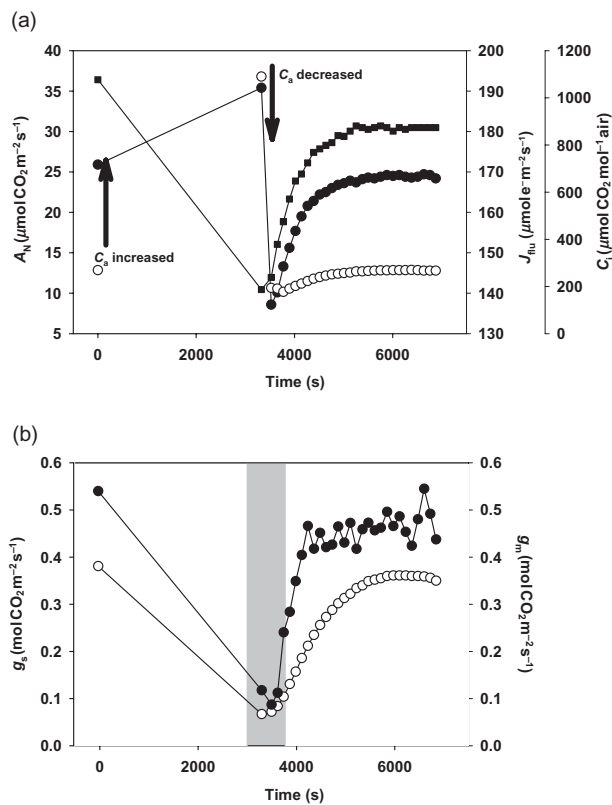


**Figure 6.** Time-course of (a) net photosynthesis ( $A_N$ , filled circles), electron transport rate ( $J_{\text{flu}}$ , filled squares) and sub-stomatal  $\text{CO}_2$  concentration ( $C_i$ , empty circles), and (b) stomatal ( $g_s$ , empty circles) and mesophyll conductance ( $g_m$ , filled circles) in *Nicotiana glauca* subjected to changes in  $\text{CO}_2$  concentrations in the atmosphere ( $C_a$ ) from 400 to 1500  $\mu\text{mol CO}_2 \text{ mol}^{-1}$  air and back (indicated with arrows in panel A). A single experiment representative of a series of similar ones is shown. Un-shaded regions indicate  $g_m$  data with a  $dC_i/dA_N$  between 10 and 50, which are reliable according to Harley *et al.* (1992).

in leaves of *N. sylvestris* to determine  $g_m$  by online carbon isotope discrimination at two different  $\text{CO}_2$  concentrations, 400 and 1000  $\mu\text{mol CO}_2 \text{ mol}^{-1}$  air, in atmospheres containing either 21 or 1%  $\text{O}_2$  (Table 2). The values obtained for  $\delta^{13}\text{C}_o - \delta^{13}\text{C}_c$  and  $\Delta^{13}\text{C}_{\text{obs}}$  were similar to those in the previous experiment, and did not differ significantly in the absence of  $\text{O}_2$  (Table 2). The results confirmed a decline of  $g_m$  at high  $\text{CO}_2$ , and no significant differences at  $P < 0.05$  were observed when measurements were taken at 21 or 1%  $\text{O}_2$  (Table 2), thus suggesting that discrimination during photorespiration can be neglected for  $g_m$  estimations.

An additional independent method, consisting in a novel curve-fitting of  $A_N$ - $C_i$  curves was applied. This method allows solving  $g_m$  at the two different regions of the curves (Ethier & Livingston 2004; Ethier *et al.* 2006), that is, together with  $V_{c,\text{max}}$  when photosynthesis is limited by carboxylation ( $g_m V_{c,\text{max}}$ ), and with  $J_{\text{max}}$  when it is limited by RuBP regeneration ( $g_m J_{\text{max}}$ ). In three of the species (*Nicotiana*, *Limonium* and *Olea*), a few additional  $A_N$ - $C_i$  curves were performed to include a larger number of points (i.e. different  $C_a$ ), allowing the application of this method. In

*Arabidopsis*, the method could be applied using the same curves as for fluorescence. Clearly, this method also supported that  $g_m$  varies along the  $C_i$  gradient during  $A_N$ - $C_i$  curves. In fact, averaging fluorescence-derived  $g_m$  values from Fig. 3 for each  $C_i$  region in each species resulted in a highly significant correlation with values estimated using the curve-fitting method (Fig. 7).

## DISCUSSION

Although rapid changes of  $g_m$  in response to  $\text{CO}_2$  have previously been suggested (Centritto *et al.* 2003; Düring 2003), no detailed analysis of this response has yet been performed. The present data show, in six different species, that  $g_m$  varies in the short term (minutes) by as much as five- to ninefold in response to changes in  $C_i$  between 50 and 1200  $\mu\text{mol CO}_2 \text{ mol}^{-1}$  air, that is, well within the timing and values generally used during the performance of  $A_N$ - $C_i$  curves.  $g_m$  strongly declines at high  $C_i$ , that is, when photosynthesis is no longer limited by  $\text{CO}_2$  availability. This response has been confirmed modifying the timing and conditions during  $A_N$ - $C_i$  curves, as well as by two totally independent methods for  $g_m$  estimation, that is, online carbon isotope discrimination method (Evans *et al.* 1986) and the curve-fitting method (Ethier & Livingston 2004; Ethier *et al.* 2006). Recently, we have been informed that similar results have been obtained by two other research groups (Ethier and Pepin, personal communication; Warren, personal communication).

Using three totally independent methods, based on different assumptions, which show similar results decreases the possibility that the observed  $g_m$  variations with  $\text{CO}_2$  are due to artefacts during gas-exchange measurements or result from misleading estimations of the parameters involved in the calculations, particularly when using the fluorescence method. Several limitations of current portable gas-exchange systems have been considered and studied (Long & Bernacchi 2003): lateral leakage inside and outside the chamber which was determined and used to correct values (Flexas *et al.* 2007), lateral  $\text{CO}_2$  diffusion outside and inside the leaf between the darkened area of the leaf under the chamber gasket and the leaf area of the light, although difficult to quantify, is considered to be minor especially when measurements are done at high light intensity (Jahnke & Krewitt 2002; Galmés *et al.* 2006). Regarding the parameters involved in  $g_m$  calculations using the fluorescence method, the critical assumptions are: day respiration ( $R_d$ ),  $\text{CO}_2$  photocompensation point ( $\Gamma^*$ ), leaf absorbance ( $\alpha$ ), light partitioning between photosystems ( $\beta$ ) and the absence of alternative electron-consuming reactions, such as the Mehler reaction. The fact that the relationship between  $\phi_{\text{PSII}}$  and  $\phi_{\text{CO}_2}$  under low  $\text{O}_2$  was similar when changing light intensity or  $\text{CO}_2$  concentrations (see Fig. 1) suggests that  $\alpha$  and  $\beta$  were not affected by  $\text{CO}_2$  concentration. However, in addition to photosynthesis and photorespiration, other reactions such as the Mehler reaction or nitrite reduction have been shown to consume as much as 10% of the total  $J_{\text{flu}}$  (Miyake & Yokota 2000; Laisk



	$C_a$ (400 $\mu\text{mol CO}_2$ $\text{mol}^{-1}$ air)	$C_a$ (1500 $\mu\text{mol CO}_2$ $\text{mol}^{-1}$ air)
$A_N$ ( $\mu\text{mol CO}_2 \text{ m}^{-2} \text{ s}^{-1}$ )	18.9 $\pm$ 1.1	29.3 $\pm$ 1.0
$g_s$ ( $\text{mol CO}_2 \text{ m}^{-2} \text{ s}^{-1}$ )	0.228 $\pm$ 0.021	0.128 $\pm$ 0.023
$\delta^{13}\text{C}_o - \delta^{13}\text{C}_c$ (‰)	0.86 $\pm$ 0.05	0.44 $\pm$ 0.04
$\Delta^{13}\text{C}_{\text{obs}}$ (‰)	12.4 $\pm$ 0.7	16.7 $\pm$ 1.2
$g_m$ Harley ( $\text{mol CO}_2 \text{ m}^{-2} \text{ s}^{-1}$ )	0.213 $\pm$ 0.018	0.053 $\pm$ 0.012
$g_m$ Evans ( $\text{mol CO}_2 \text{ m}^{-2} \text{ s}^{-1}$ )	0.192 $\pm$ 0.010	0.088 $\pm$ 0.011
$C_i$ ( $\mu\text{mol CO}_2 \text{ mol}^{-1}$ air)	275 $\pm$ 9	1145 $\pm$ 62
$C_c$ ( $\mu\text{mol CO}_2 \text{ mol}^{-1}$ air)	170 $\pm$ 17	792 $\pm$ 72

$g_m$  was estimated by two independent methods, a gas-exchange–chlorophyll fluorescence method ( $g_m$  Harley) and online carbon isotope discrimination method ( $g_m$  Evans). Values are averages  $\pm$  SE of five replicates per  $\text{CO}_2$  concentration. The  $C_c$  shown was calculated using the  $g_m$  values obtained using the Harley method.

*et al.* 2006), and their incidence can be higher at ambient than at high  $\text{CO}_2$  concentration (Miyake & Yokota 2000). Moreover,  $R_d$  may be underestimated when using the Laisk method (Pinelli & Loreto 2003), and high  $\text{CO}_2$  has been sometimes reported to substantially reduce  $R_d$  (Gonzalez-Meler *et al.* 1996; Bruhn, Wiskich & Atkin 2007). Finally, using  $C_i^*$  instead of  $\Gamma^*$  may lead to further errors. These two parameters relate to each other following the equation:  $\Gamma^* = C_i^* + R_d/g_m$ . As explained in M&M,  $g_m$  was not estimated close to the compensation point, and hence  $C_i^*$  was used as a proxy for  $\Gamma^*$ . To assess the possibility that our conclusions were due to the interference of the possible bias in assumed parameters, their effects on  $g_m$  for several leaves of the different species were simulated.

An example of such simulations is shown in Table 3 for a leaf of *Arabidopsis* (simulations for other species resulted in qualitatively similar results, not shown). At ambient (400  $\mu\text{mol CO}_2 \text{ mol}^{-1}$  air) and high (1500  $\mu\text{mol CO}_2 \text{ mol}^{-1}$  air)  $\text{CO}_2$ , respectively, leaf temperature was 25.2 and 25.7 °C,  $A_N$  was 13.0 and 23.0  $\mu\text{mol CO}_2 \text{ m}^{-2} \text{ s}^{-1}$ ,  $C_i$  was 283 and 1165  $\mu\text{mol CO}_2 \text{ mol}^{-1}$  air, and  $J_{\text{flu}}$  was 112 and 125  $\mu\text{mol e}^- \text{ m}^{-2} \text{ s}^{-1}$ . Using these data, together with estimations of  $R_d$  ( $-0.46 \mu\text{mol CO}_2 \text{ m}^{-2} \text{ s}^{-1}$ ) and  $C_i^*$  (44  $\mu\text{mol CO}_2 \text{ mol}^{-1}$  air, used as a proxy for  $\Gamma^*$ ) obtained from the Laisk method resulted in  $g_m$  estimates of 0.110 and

0.032  $\mu\text{mol CO}_2 \text{ m}^{-2} \text{ s}^{-1}$  at ambient and high  $\text{CO}_2$ , respectively. Regarding the possible influence of alternative electron-consuming reactions, two simulations were performed (Table 3). In the first, these reactions were considered to consume 10% of total  $J_{\text{flu}}$  (Miyake & Yokota 2000; Laisk *et al.* 2006), while in the second it was considered that these reactions were present at ambient but negligible at high  $\text{CO}_2$  concentration (Miyake & Yokota 2000). With respect to respiration (Table 3), two possibilities were considered: (1) that the actual  $R_d$  was about twice the estimated one (i.e. close to  $R_N$ , as suggested by Pinelli & Loreto 2003) and (2) that at high  $\text{CO}_2$ ,  $R_D$  would be reduced by 30% (Gonzalez-Meler *et al.* 1996; Bruhn *et al.* 2007). With regard to  $\Gamma^*$ , although no estimation of  $g_m$  at the compensation point was made, judging from Fig. 3,  $g_m$  at the compensation point could be either low (around 0.1  $\mu\text{mol CO}_2 \text{ m}^{-2} \text{ s}^{-1}$  in most species) or high (between 0.2 and 0.6  $\mu\text{mol CO}_2 \text{ m}^{-2} \text{ s}^{-1}$ , averaging 0.4). Therefore, two simulations were performed (Table 3). In the first,  $g_m$  at near the compensation point was assumed to be 0.1  $\mu\text{mol CO}_2 \text{ m}^{-2} \text{ s}^{-1}$ , resulting in a  $\Gamma^*$  of 58.3  $\mu\text{mol CO}_2 \text{ mol}^{-1}$  air. In the second,  $g_m$  near the compensation point was assumed to be 0.4  $\mu\text{mol CO}_2 \text{ m}^{-2} \text{ s}^{-1}$ , resulting in a  $\Gamma^*$  of 46.4  $\mu\text{mol CO}_2 \text{ mol}^{-1}$  air. Because  $\Gamma^*$  reflects an intrinsic property of Rubisco, it may be equal at ambient and high  $\text{CO}_2$ . At ambient  $\text{CO}_2$ , all the simulated values ranged

**Table 2.** Net photosynthesis ( $A_N$ ), stomatal conductance ( $g_s$ ), mesophyll conductance ( $g_m$ ), sub-stomatal ( $C_i$ ) and chloroplast ( $C_c$ )  $\text{CO}_2$  concentrations, the difference in  $\delta^{13}\text{C}$  between the air leaving and entering the leaf cuvette ( $\delta^{13}\text{C}_o - \delta^{13}\text{C}_c$ ) and the observed  $^{13}\text{C}$  discrimination ( $\Delta^{13}\text{C}_{\text{obs}}$ ) by leaves of *Nicotiana sylvestris* acclimated for 15 min to either 400 or 1000  $\mu\text{mol CO}_2 \text{ mol}^{-1}$  air, and in an atmosphere containing 21 or 1%  $\text{O}_2$

	$C_a$ (400 $\mu\text{mol CO}_2$ $\text{mol}^{-1}$ air) 21% $\text{O}_2$	$C_a$ (1000 $\mu\text{mol CO}_2$ $\text{mol}^{-1}$ air) 21% $\text{O}_2$	$C_a$ (400 $\mu\text{mol CO}_2$ $\text{mol}^{-1}$ air) 1% $\text{O}_2$	$C_a$ (1000 $\mu\text{mol CO}_2$ $\text{mol}^{-1}$ air) 1% $\text{O}_2$
$A_N$ ( $\mu\text{mol CO}_2 \text{ m}^{-2} \text{ s}^{-1}$ )	14.0 $\pm$ 0.4	22.6 $\pm$ 0.8	17.9 $\pm$ 1.4	22.7 $\pm$ 0.7
$g_s$ ( $\text{mol CO}_2 \text{ m}^{-2} \text{ s}^{-1}$ )	0.192 $\pm$ 0.010	0.093 $\pm$ 0.005	0.184 $\pm$ 0.024	0.075 $\pm$ 0.002
$\delta^{13}\text{C}_o - \delta^{13}\text{C}_c$ (‰)	0.71 $\pm$ 0.02	0.39 $\pm$ 0.02	0.71 $\pm$ 0.08	0.32 $\pm$ 0.02
$\Delta^{13}\text{C}_{\text{obs}}$ (‰)	15.8 $\pm$ 0.9	13.7 $\pm$ 0.3	12.4 $\pm$ 0.7	11.2 $\pm$ 0.9
$g_m$ ( $\text{mol CO}_2 \text{ m}^{-2} \text{ s}^{-1}$ )	0.267 $\pm$ 0.034	0.177 $\pm$ 0.055	0.300 $\pm$ 0.037	0.152 $\pm$ 0.016
$C_i$ ( $\mu\text{mol CO}_2 \text{ mol}^{-1}$ air)	249 $\pm$ 5	545 $\pm$ 35	199 $\pm$ 11	451 $\pm$ 14
$C_c$ ( $\mu\text{mol CO}_2 \text{ mol}^{-1}$ air)	192 $\pm$ 9	395 $\pm$ 10	137 $\pm$ 11	293 $\pm$ 32

$g_m$  was estimated by online carbon isotope discrimination method. Values are averages  $\pm$  SE of five replicates per  $\text{CO}_2$  concentration.

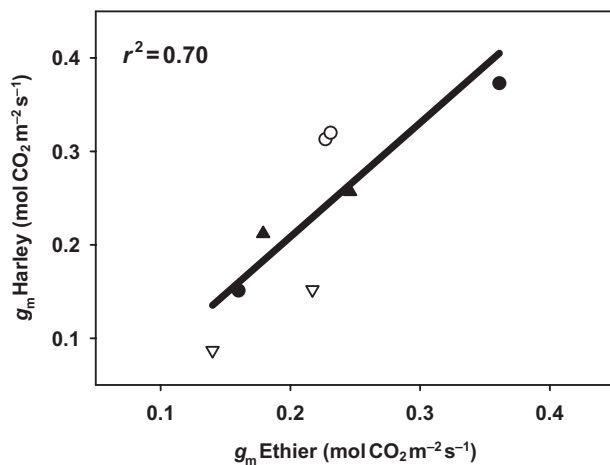


**Figure 7.** Relationship between estimates of mesophyll conductance ( $g_m$ ) by combined gas exchange and chlorophyll fluorescence ( $g_m$  Harley) and the curve-fitting method ( $g_m$  Ethier) at different regions of net photosynthesis and sub-stomatal CO<sub>2</sub> concentration ( $A_N-C_i$ ) curves [maximum carboxylation capacity ( $V_{c,max}$ ), maximum capacity for electron transport rate ( $J_{max}$ )]. For the Harley method, all values of  $g_m$  shown in Fig. 2 within each interval were averaged to get an 'average'  $g_m$  for each region. Notice that estimates by the two methods were made in the same species and  $C_i$  intervals, but not in the same leaves and measuring time.

between 0.118 and 0.145  $\mu\text{mol CO}_2 \text{ m}^{-2} \text{ s}^{-1}$  (i.e. close to the original estimation of 0.110  $\mu\text{mol CO}_2 \text{ m}^{-2} \text{ s}^{-1}$ ) except when a  $\Gamma^*$  of 58.3  $\mu\text{mol CO}_2 \text{ mol}^{-1}$  air was considered, which yielded a much higher  $g_m$  (0.317  $\mu\text{mol CO}_2 \text{ m}^{-2} \text{ s}^{-1}$ ). However, the latter value is unlikely, because a  $\Gamma^*$  of 58.3  $\mu\text{mol CO}_2 \text{ mol}^{-1}$  would reflect a specificity factor of only 64, that is, the lowest by far ever described for a C<sub>3</sub> species (Galmés *et al.* 2005). In addition, at high CO<sub>2</sub>, all the simulated values ranged between 0.031 and 0.050  $\mu\text{mol CO}_2 \text{ m}^{-2} \text{ s}^{-1}$ . Therefore, although misleading assumptions in any of the parameters involved in  $g_m$  calculations may lead to variations in the absolute values of estimated  $g_m$ , none of them would impair the conclusion that  $g_m$  declines at high CO<sub>2</sub>. In the case of the isotope method, the major limitation would be the interference of carbon isotope discrimination during photorespiration (Ghashghaie *et al.* 2003), which may be substantially different at ambient and high CO<sub>2</sub>. However, the fact that similar  $g_m$  estimations were obtained under 21 and 1% O<sub>2</sub> regardless of CO<sub>2</sub> concentration, suggests that the interference of photorespiration does not affect  $g_m$  estimations. Altogether, it provides convincing evidence that decreased  $g_m$  at high CO<sub>2</sub> has a physiological basis, and does not result from artefacts in the methods used for its estimation.

Except for the species-dependent differences at low  $C_i$ , the response of  $g_m$  to increasing  $C_i$  resembles that known for  $g_s$  (Raschke 1979). Moreover, these data suggest that  $g_m$  responds faster to varying  $C_i$  than does  $g_s$ . The data shown in Fig. 5 suggest that, as observed for  $g_s$ ,  $g_m$  responds to changes in light intensity, although further studies are needed. Together, decreasing  $g_s$  and  $g_m$  as  $C_i$  increases

strongly reduces the chloroplast CO<sub>2</sub> concentration ( $C_c$ ) with respect to ambient ( $C_a$ ), particularly at high CO<sub>2</sub> concentrations. The function of this regulation is unknown, and can only be speculated. One possibility is that this response serves to match CO<sub>2</sub> availability and photosynthetic capacity. When photosynthesis is limited by CO<sub>2</sub> availability,  $g_m$  tends to be higher (with some exceptions at low  $C_i$ ), which may result in increased CO<sub>2</sub> availability in the chloroplast stroma. Consequently,  $g_m$  decreases when photosynthesis is no longer limited by CO<sub>2</sub> availability, that is, at high  $C_i$ , which may explain also why it seems to be lower when light is limiting photosynthesis (Fig. 5). A sustained high  $g_m$  at high  $C_i$ , when photosynthesis cannot increase the rate of CO<sub>2</sub> consumption, would almost double the CO<sub>2</sub> concentration in the chloroplast stroma ( $C_c$ ) according to  $C_i/C_a$  and  $C_c/C_a$  ratios. Maintaining both  $g_s$  and  $g_m$  high would result in about fourfold increase in  $C_c$ . According to the known relationship between CO<sub>2</sub> concentration in water and pH, this could result in a significant decrease of stromal pH (up to about 0.3 to 0.5 units if stromal content is assumed to be pure water), which could be detrimental to photosynthesis due to the extreme pH sensitivity of photosynthetic enzymes (Berkowitz, Chen & Gibbs 1983; Pfanz 1995). While this possibility cannot be discarded at present, it is unlikely because efficient pH regulation mechanisms have been shown to operate in chloroplasts (Hauser *et al.* 1995; Oja *et al.* 1999; Savchenko *et al.* 2000). Alternatively, perhaps the mechanism leading to a high  $g_m$  requires energy, although this is unknown at present (see further discussion). If so, at high CO<sub>2</sub> where photosynthesis is limited by energy availability, increasing  $g_m$  would compete with photosynthesis for energy, and would be inefficient as the added CO<sub>2</sub> reaching the chloroplast would result in little increase of CO<sub>2</sub> fixation. The opposite would be true at low CO<sub>2</sub>, that is, energy is in excess to that required for photosynthesis, and increased CO<sub>2</sub> availability would be beneficial for photosynthesis.

Despite substantial knowledge about the regulation of stomatal opening, the mechanisms leading to its response to  $C_i$  are still unclear. It has been hypothesized that these may be related to malate-induced regulation of anion channels (Hedrich *et al.* 1994), to CO<sub>2</sub>-related pH and membrane potential changes in guard cells (Hedrich *et al.* 2001), or to CO<sub>2</sub>-mediated changes in photosynthesis in guard cells (Messinger, Buckley & Mott 2006), in a mechanism mediated either by zeaxanthin (Zeiger *et al.* 2002) or ATP (Buckley, Mott & Farquhar 2003). Much less is known about the regulation of mesophyll conductance variations, and until recently it was assumed that leaf structural properties were causing most  $g_m$  variations (von Caemmerer & Evans 1991; Lloyd *et al.* 1992). One of the few physiological bases known is the recent discovery that some aquaporins can be involved in the regulation of  $g_m$  (Hanba *et al.* 2004; Flexas *et al.* 2006). Actually, transgenic tobacco plants differing in the amounts of aquaporin NtAQP1 differ in their slope of  $g_m$  response to  $C_i$  (Fig. 2), suggesting that NtAQP1 may also be involved in this response. While the responses of aquaporin physiology to

**Table 3.** Simulation of the effects of possible errors in the model parameters assumptions on mesophyll conductance ( $g_m$ ) estimates using the chlorophyll fluorescence method by Harley *et al.* (1992) in a leaf of *Arabidopsis thaliana* at 400  $\mu\text{mol CO}_2 \text{ mol}^{-1}$  air (ambient  $\text{CO}_2$ ) or 1500  $\mu\text{mol CO}_2 \text{ mol}^{-1}$  air (high  $\text{CO}_2$ )

A. Effect of possible alternative electron flow and its dependence on $\text{CO}_2$ . In the first row, alternative electron-consuming reactions are assumed to use 10% of total electron transport rate ( $J_{\text{hu}}$ ), while in the second row alternative electron-consuming reactions are assumed to use 10% of total $J_{\text{hu}}$ only at ambient $\text{CO}_2$ , being negligible at high $\text{CO}_2$ .			
$J_{\text{hu}}$ Ambient $\text{CO}_2$ ( $\mu\text{mol e}^- \text{ m}^{-2} \text{ s}^{-1}$ )	$J_{\text{hu}}$ High $\text{CO}_2$ ( $\mu\text{mol e}^- \text{ m}^{-2} \text{ s}^{-1}$ )	$g_m$ Ambient $\text{CO}_2$ ( $\mu\text{mol CO}_2 \text{ m}^{-2} \text{ s}^{-1}$ )	$g_m$ High $\text{CO}_2$ ( $\mu\text{mol CO}_2 \text{ m}^{-2} \text{ s}^{-1}$ )
101	113	0.145	0.050
101	125	0.145	0.032
B. Effect of possible misleading estimates of $R_d$ and its dependence on $\text{CO}_2$ . In the first row, $R_d$ is assumed to be equal to respiration in the dark ( $R_N$ ). In the second row, in addition, $R_d$ at high $\text{CO}_2$ is assumed to be only 30% that at low $\text{CO}_2$ .			
$R_d$ Ambient $\text{CO}_2$ ( $\mu\text{mol CO}_2 \text{ m}^{-2} \text{ s}^{-1}$ )	$R_d$ High $\text{CO}_2$ ( $\mu\text{mol CO}_2 \text{ m}^{-2} \text{ s}^{-1}$ )	$g_m$ Ambient $\text{CO}_2$ ( $\mu\text{mol CO}_2 \text{ m}^{-2} \text{ s}^{-1}$ )	$g_m$ High $\text{CO}_2$ ( $\mu\text{mol CO}_2 \text{ m}^{-2} \text{ s}^{-1}$ )
0.92	0.92	0.118	0.033
0.92	0.31	0.118	0.031
C. Effect of using apparent $\text{CO}_2$ photocompensation point ( $C_i^*$ ) instead of chloroplastic $\text{CO}_2$ photocompensation point ( $\Gamma^*$ ). Two estimations are made. In the first row, $g_m$ near the compensation point is assumed to be 0.1 $\mu\text{mol CO}_2 \text{ m}^{-2} \text{ s}^{-1}$ , resulting in a $\Gamma^*$ of 58.3 $\mu\text{mol CO}_2 \text{ mol}^{-1}$ air. In the second row, $g_m$ near the compensation point is assumed to be 0.4 $\mu\text{mol CO}_2 \text{ m}^{-2} \text{ s}^{-1}$ , resulting in a $\Gamma^*$ of 46.4 $\mu\text{mol CO}_2 \text{ mol}^{-1}$ air.			
$\Gamma^*$ Ambient $\text{CO}_2$ ( $\mu\text{mol CO}_2 \text{ mol}^{-1}$ air)	$\Gamma^*$ High $\text{CO}_2$ ( $\mu\text{mol CO}_2 \text{ mol}^{-1}$ air)	$g_m$ Ambient $\text{CO}_2$ ( $\mu\text{mol CO}_2 \text{ m}^{-2} \text{ s}^{-1}$ )	$g_m$ High $\text{CO}_2$ ( $\mu\text{mol CO}_2 \text{ m}^{-2} \text{ s}^{-1}$ )
58.3	58.3	0.317	0.047
46.4	46.4	0.144	0.037

varying CO<sub>2</sub> have not been studied, it has been shown that a change in cytosolic pH of 0.5 to 1.0 units can induce a strong gating of aquaporins through protonation of a histidine residue of the protein (Tournaire-Roux *et al.* 2003), therefore providing a potential mechanism for the observed CO<sub>2</sub>-induced regulation. In addition, an energy-dependent gating based on phosphorylation has been described (Kjellbom *et al.* 1999), which would match the energy-dependent hypothesis for  $g_m$  regulation raised earlier. An alternative mechanism, not based on aquaporin function, could be related to chloroplast swelling and shrinkage. Modifications in chloroplast shape, preventing close association between chloroplast and cell surface, have been shown to alter  $g_m$  in phytochrome mutants of tobacco (Sharkey *et al.* 1991). Moreover,  $g_m$  could be affected by chloroplast swelling or movements (Sharkey, personal communication; Tholen *et al.* (2007). Whether this occurs under high CO<sub>2</sub> remains unknown. Clearly, further studies would be needed to elucidate which mechanisms can mediate  $g_m$  responses to CO<sub>2</sub>.

Regardless of the physiological reasons for and the mechanisms involved in the regulation of the response of  $g_m$  to CO<sub>2</sub>, the observed variations during the performance of typical  $A_N$ -C<sub>i</sub> curves may induce errors on the photosynthesis parameterization. These  $A_N$ -C<sub>i</sub> curves are commonly used to develop prediction models of CO<sub>2</sub> assimilation for crops (Díaz-Espejo *et al.* 2006) and natural vegetation (Xu & Baldocchi 2003), to help predicting the effects of climate change on photosynthesis (Rogers *et al.* 2001), for scaling up from leaf to whole plant and/or ecosystem carbon assimilation models (Harley & Baldocchi 1995), and to assess the influence of stresses on the photosynthetic capacity of plants (Centritto *et al.* 2003; Loreto *et al.* 2003). Therefore, its correct parameterization is important, and this should take into account mesophyll conductance to CO<sub>2</sub>, as already highlighted (Ethier & Livingston 2004). However,  $A_N$ -C<sub>i</sub> curves are often transformed to  $A_N$ -C<sub>e</sub> curves using a value for  $g_m$  determined at ambient CO<sub>2</sub> and assuming a constant  $g_m$  for the entire range of C<sub>i</sub> (Flexas *et al.* 2002; Manter & Kerrigan 2004; Grassi & Magnani 2005; Galmés *et al.* 2006), which may not be true according to the present results. The effect of neglecting changes of  $g_m$  with varying C<sub>i</sub> on parameterization of  $A_N$ -C<sub>e</sub> curves is illustrated with a few examples in Fig. 8. In some cases, when  $g_m$  is large, like in *Arabidopsis* (Fig. 8a) or *Vitis* (Fig. 8b), the  $A_N$ -C<sub>e</sub> curve determined by concomitant gas-exchange and chlorophyll fluorescence measurements along the entire range of C<sub>a</sub> differs from that estimated from a single  $g_m$  value at ambient CO<sub>2</sub> mostly on the maximum value of C<sub>e</sub> attained, while the differences in parameterization of V<sub>c,max</sub> and J<sub>max</sub> are negligible. In other cases, however, when  $g_m$  is largely reduced, such as under severe water stress, the effect is expected to be substantial, because the difference between C<sub>i</sub> and C<sub>e</sub> becomes greater. This is illustrated by the response of a *Vitis* leaf subjected to severe water stress (Fig. 8c). Assuming a constant  $g_m$  may have led to an estimation of V<sub>c,max</sub> of only 19  $\mu\text{mol m}^{-2} \text{s}^{-1}$ , accompanied by a very low J<sub>max</sub>. However, taking into account the variations of

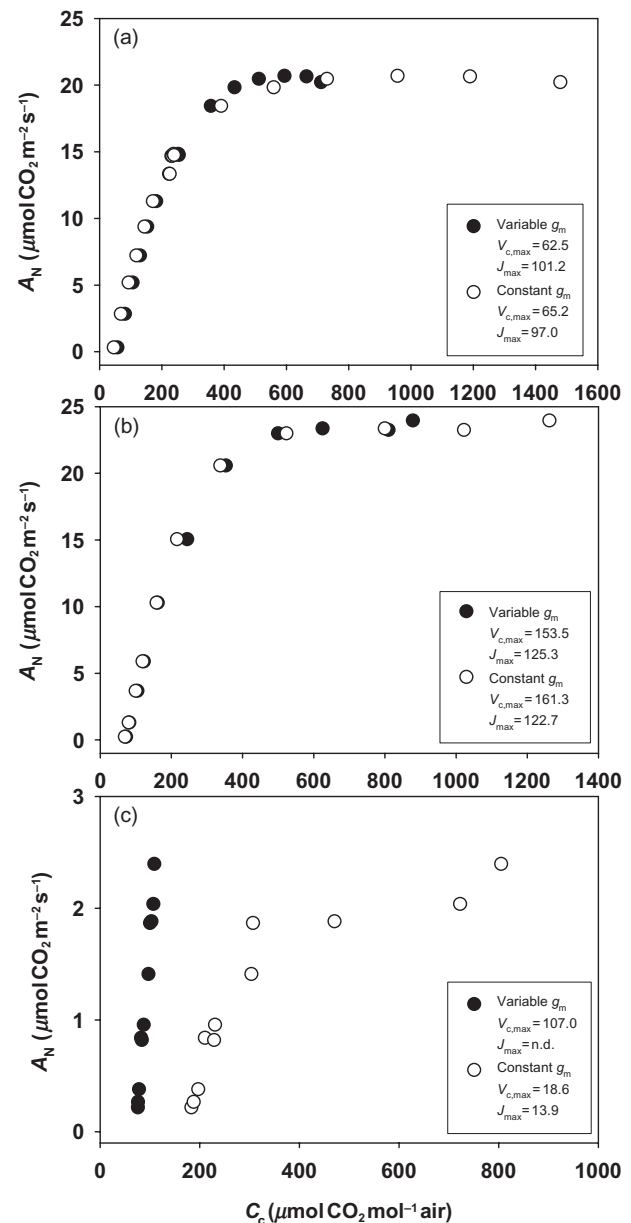


**Figure 8.** Examples of the effects of neglecting mesophyll conductance ( $g_m$ ) variations with sub-stomatal CO<sub>2</sub> concentration ( $C_i$ ) on the parameterization of  $A_N$ -C<sub>e</sub> curves.  $A_N$ -C<sub>e</sub> curves were determined by concomitant gas-exchange and chlorophyll fluorescence measurements along the entire range of CO<sub>2</sub> concentrations in the atmosphere ( $C_a$ , filled circles) or from a single  $g_m$  value determined at ambient CO<sub>2</sub> (empty circles). The curves shown are for well-irrigated *Arabidopsis* (a), a well-irrigated *Vitis* (b) and a severely water-stressed *Vitis* (c). At 400  $\mu\text{mol CO}_2 \text{ mol}^{-1} \text{ air}$ , estimated  $g_m$  values were 0.200, 0.291 and 0.005  $\mu\text{mol CO}_2 \text{ m}^{-2} \text{ s}^{-1}$  for *Arabidopsis*, irrigated *Vitis* and stressed *Vitis*, respectively. Values of maximum carboxylation capacity ( $V_{c,max}$ ) and maximum capacity for electron transport rate ( $J_{max}$ ) estimated for each curve are shown in the inset.

$g_m$  with  $C_i$  results in an estimation of  $V_{c,max}$  of up to  $107 \text{ mol m}^{-2} \text{ s}^{-1}$ , that is, only slightly depressed as compared to the irrigated plant, while  $J_{max}$  cannot be determined. The latter result matches better biochemical evidence in water-stressed plants (Flexas *et al.* 2004).

## CONCLUSION

In conclusion, the present study clearly demonstrates that mesophyll conductance to  $\text{CO}_2$  changes in response to varying  $\text{CO}_2$  even faster than does stomatal conductance, and this should be taken into account for a correct parameterization of  $A_N-C_i$  curves, particularly when  $g_m$  is low as, for instance, under stress. These results are striking and urge the need for studies regarding both the function and the physiological and molecular basis of such regulation.

## ACKNOWLEDGMENTS

This work was granted by project BFU2005-03102/BFI (Plan Nacional, Spain). M. Ribas-Carbo and A. Díaz-Espejo were beneficiaries of the 'Programa Ramón y Cajal' (M.E.C.). We would like to thank Dr Biel Martorell for his technical help on the IRMS and all the staff at the Serveis Científico-Tècnics of the Universitat de les Illes Balears for their help with measurements with mass spectrometer. Helpful discussions with Drs T.D. Sharkey, F. Loreto and B. Vilanova are gratefully acknowledged.

## REFERENCES

- Berkowitz G.A., Chen C. & Gibbs M. (1983) Stromal acidification mediates in vivo water stress inhibition of non-stomatal-controlled photosynthesis. *Plant Physiology* **72**, 1123–1126.
- Bernacchi C.J., Portis A.R., Nakano H., von Caemmerer S. & Long S.P. (2002) Temperature response of mesophyll conductance. Implications for the determination of Rubisco enzyme kinetics and for limitations to photosynthesis in vivo. *Plant Physiology* **130**, 1992–1998.
- Bernacchi C.J., Morgan P.B., Ort D.R. & Long S.P. (2005) The growth of soybean under free air  $[\text{CO}_2]$  enrichment (FACE) stimulates photosynthesis while decreasing in vivo Rubisco capacity. *Planta* **220**, 434–446.
- Bongi G. & Loreto F. (1989) Gas-exchange properties of salt-stressed olive (*Olea europaea* L.) leaves. *Plant Physiology* **90**, 1408–1416.
- Bruhn D., Wiskich J.T. & Atkin O.K. (2007) Contrasting responses by respiration to elevated  $\text{CO}_2$  in intact tissue and isolated mitochondria. *Functional Plant Biology* **34**, 112–117.
- Buckley T.N., Mott K.A. & Farquhar G.D. (2003) A hydromechanical and biochemical model of stomatal conductance. *Plant, Cell & Environment* **26**, 1767–1786.
- von Caemmerer S. (2000) *Biochemical Model of Leaf Photosynthesis*. CSIRO Publishing, Canberra, Australia.
- von Caemmerer S. & Evans J.R. (1991) Determination of the average partial pressure of  $\text{CO}_2$  in chloroplasts from leaves of several  $\text{C}_3$  plants. *Australian Journal of Plant Physiology* **18**, 287–305.
- Centritto M., Loreto F. & Chartzoulakis K. (2003) The use of low  $[\text{CO}_2]$  to estimate diffusional and non-diffusional limitations of photosynthetic capacity of salt-stressed olive samplings. *Plant, Cell & Environment* **26**, 585–594.
- Di Marco G., Manes F., Tricoli D. & Vitale E. (1990) Fluorescence parameters measured concurrently with net photosynthesis to investigate chloroplastic  $\text{CO}_2$  concentration in leaves of *Quercus ilex* L. *Journal of Plant Physiology* **136**, 538–543.
- Díaz-Espejo A., Walcroft A.S., Fernández J.E., Hafidi B., Palomo M.J. & Girón I.F. (2006) Modelling photosynthesis in olive leaves under drought conditions. *Tree Physiology* **26**, 1445–1456.
- Düring H. (2003) Stomatal and mesophyll conductances to  $\text{CO}_2$  transfer to chloroplasts in leaves of grapevine (*Vitis vinifera* L.). *Vitis* **42**, 65–68.
- Eckert M., Biela A., Siefritz F. & Kaldenhoff R. (1999) New aspects of plant aquaporin regulation and specificity. *Journal of Experimental Botany* **50**, 1541–1545.
- Ethier G.H. & Livingston N.J. (2004) On the need to incorporate sensitivity to  $\text{CO}_2$  transfer conductance into the Farquhar–von Caemmerer–Berry leaf photosynthesis model. *Plant, Cell & Environment* **27**, 137–153.
- Ethier G.H., Livingston N.J., Harrison D.L., Black T.A. & Moran J.A. (2006) Low stomatal and internal conductance to  $\text{CO}_2$  versus Rubisco deactivation as determinants of the photosynthetic decline of ageing evergreen leaves. *Plant, Cell & Environment* **29**, 2168–2184.
- Evans J.R. & von Caemmerer S. (1996) Carbon dioxide diffusion inside leaves. *Plant Physiology* **110**, 339–346.
- Evans J.R., Sharkey T.D., Berry J.A. & Farquhar G.D. (1986) Carbon isotope discrimination measured concurrently with gas exchange to investigate  $\text{CO}_2$  diffusion in leaves of higher plants. *Australian Journal of Plant Physiology* **13**, 281–292.
- Farquhar G.D., von Caemmerer S. & Berry J.A. (1980) A biochemical model of photosynthetic  $\text{CO}_2$  assimilation in leaves of  $\text{C}_3$  species. *Planta* **149**, 78–90.
- Flexas J., Bota J., Escalona J.M., Sampol B. & Medrano H. (2002) Effects of drought on photosynthesis in grapevines under field conditions: an evaluation of stomatal and mesophyll limitations. *Functional Plant Biology* **29**, 461–471.
- Flexas J., Bota J., Loreto F., Cornic G. & Sharkey T.D. (2004) Diffusive and metabolic limitations to photosynthesis under drought and salinity in  $\text{C}_3$  plants. *Plant Biology* **6**, 269–279.
- Flexas J., Ribas-Carbó M., Hanson D.T., Bota J., Otto B., Cifre J., McDowell N., Medrano H. & Kaldenhoff R. (2006) Tobacco aquaporin NtAQP1 is involved in mesophyll conductance to  $\text{CO}_2$  in vivo. *Plant Journal* **48**, 427–439.
- Flexas J., Díaz-Espejo A., Berry J.A., Galmés J., Cifre J., Kaldenhoff R., Medrano H. & Ribas-Carbó M. (2007) Leakage in leaf chambers in open gas exchange systems: quantification and its effects in photosynthesis parameterization. *Journal of Experimental Botany* **58**, 1533–1543.
- Galmés J., Flexas J., Keys A.J., Cifre J., Mitchell R.A.C., Madgwick P.J., Haslam R.P., Medrano H. & Parry M.A.J. (2005) Rubisco specificity factor tends to be larger in plant species from drier habitats and in species with persistent leaves. *Plant, Cell & Environment* **28**, 571–579.
- Galmés J., Medrano H. & Flexas J. (2006) Acclimation of Rubisco specificity factor to drought in tobacco: discrepancies between *in vitro* and *in vivo* estimations. *Journal of Experimental Botany* **57**, 3659–3667.
- Genty B., Briantais J.M. & Baker N.R. (1989) The relationship between the quantum yield of photosynthetic electron transport and quenching of chlorophyll fluorescence. *Biochimica et Biophysica Acta* **990**, 87–92.
- Ghashghaie J., Badeck F., Lanigan G., Nogues S., Tcherkez G., Deleens E., Cornic G. & Griffiths H. (2003) Carbon isotope fractionation during dark respiration and photorespiration. *Phytochemistry Reviews* **2**, 145–162.

- Gonzalez-Meler M.A., Ribas-Carbo M., Siedow J.N. & Drake B.G. (1996) Direct inhibition of plant mitochondrial respiration by elevated CO<sub>2</sub>. *Plant Physiology* **112**, 1349–1355.
- Grassi G. & Magnani F. (2005) Stomatal, mesophyll conductance and biochemical limitations to photosynthesis as affected by drought and leaf ontogeny in ash and oak trees. *Plant, Cell & Environment* **28**, 834–849.
- Hanba Y.T., Kogami H. & Terashima I. (2002) The effect of growth irradiance on leaf anatomy and photosynthesis in *Acer* species differing in light demand. *Plant, Cell & Environment* **25**, 1021–1030.
- Hanba Y.T., Shibasaka M., Hayashi Y., Hayakawa T., Kasamo K., Terashima I. & Katsuhara M. (2004) Overexpression of the barley aquaporin HvPIP2;1 increases internal CO<sub>2</sub> conductance and CO<sub>2</sub> assimilation in the leaves of transgenic rice plants. *Plant and Cell Physiology* **45**, 521–529.
- Harley P.C. & Baldocchi D.D. (1995) Scaling carbon dioxide and water vapour exchange from leaf to canopy in a deciduous forest. I. Leaf model parametrization. *Plant, Cell & Environment* **18**, 1146–1156.
- Harley P.C., Loreto F., Di Marco G. & Sharkey T.D. (1992) Theoretical considerations when estimating the mesophyll conductance to CO<sub>2</sub> flux by the analysis of the response of photosynthesis to CO<sub>2</sub>. *Plant Physiology* **98**, 1429–1436.
- Hauser M., Eichelmann H., Oja V., Haber U. & Laisk A. (1995) Stimulation by light of rapid pH regulation in the chloroplast stroma in vivo as indicated by CO<sub>2</sub> solubilization in leaves. *Plant Physiology* **108**, 1059–1066.
- Hedrich R., Marten I., Lohse G., Dietrich P., Winter H., Lohaus G. & Heldt H.W. (1994) Malate-sensitive anion channels enable guard cells to sense changes in the ambient CO<sub>2</sub>. *Plant Journal* **6**, 741–748.
- Hedrich R., Neimanis S., Savchenko G., Felle H.H., Kaiser W.M. & Heber U. (2001) Changes in apoplastic pH and membrane potential in leaves in relation to stomatal responses to CO<sub>2</sub>, malate, abscisic acid or interruption of water supply. *Planta* **213**, 594–601.
- Jahnke S. & Krewitt M. (2002) Atmospheric CO<sub>2</sub> concentration may directly affect leaf respiration measurement in tobacco, but not respiration itself. *Plant, Cell & Environment* **25**, 641–651.
- Kjellbom P., Larsson C., Johanson I., Karlsson M. & Johanson U. (1999) Aquaporins and water homeostasis in plants. *Trends in Plant Science* **4**, 308–314.
- Laisk A.K. (1977) *Kinetics of Photosynthesis and Photorespiration in C3 Plants* (in Russian). Nauka, Moscow, Russia.
- Laisk A. & Loreto F. (1996) Determining photosynthetic parameters from leaf CO<sub>2</sub> exchange and chlorophyll fluorescence. Ribulose-1,5-bisphosphate carboxylase/oxygenase specificity factor, dark respiration in the light, excitation distribution between photosystems, alternative electron transport rate, and mesophyll diffusion resistance. *Plant Physiology* **110**, 903–912.
- Laisk A., Eichelmann H., Oja V., Rasulov B. & Rämme H. (2006) Photosystem II cycle and alternative electron flow in leaves. *Plant and Cell Physiology* **47**, 972–983.
- Lloyd J., Syvertsen J.P., Kriedemann P.E. & Farquhar G.D. (1992) Low conductances for CO<sub>2</sub> diffusion from stomata to the sites of carboxylation in leaves of woody species. *Plant, Cell & Environment* **15**, 873–899.
- Long S.P. & Bernacchi C.J. (2003) Gas exchange measurements, what can they tell us about the underlying limitations to photosynthesis? Procedures and sources of error. *Journal of Experimental Botany* **54**, 2393–2401.
- Loreto F., Harley P.C., Di Marco G. & Sharkey T.D. (1992) Estimation of mesophyll conductance to CO<sub>2</sub> flux by three different methods. *Plant Physiology* **98**, 1437–1443.
- Loreto F., Di Marco G., Tricoli D. & Sharkey T.D. (1994) Measurements of mesophyll conductance, photosynthetic electron transport and alternative electron sinks of field grown wheat leaves. *Photosynthesis Research* **41**, 397–403.
- Loreto F., Centritto M. & Chartzoulakis K. (2003) Photosynthetic limitations in olive cultivars with different sensitivity to salt stress. *Plant, Cell & Environment* **26**, 595–601.
- Manter D.K. & Kerrigan J. (2004) A/C<sub>i</sub> curve analysis across a range of woody plant species: influence of regression analysis parameters and mesophyll conductance. *Journal of Experimental Botany* **55**, 2581–2588.
- Messinger S., Buckley T.N. & Mott K.A. (2006) Evidence for involvement of photosynthetic processes in the stomatal response to CO<sub>2</sub>. *Plant Physiology* **140**, 771–778.
- Miyake C. & Yokota A. (2000) Determination of the rate of photoreduction of O<sub>2</sub> in the water–water cycle in watermelon leaves and enhancement of the rate by limitation of photosynthesis. *Plant and Cell Physiology* **41**, 335–343.
- Miyazawa S.I. & Terashima I. (2001) Slow development of leaf photosynthesis in an evergreen broad-leaved tree, *Castanopsis sieboldii*: relationships between leaf anatomical characteristics and photosynthetic rate. *Plant, Cell & Environment* **24**, 279–291.
- Niinemets U., Cescatti A., Rodeghiero M. & Tosens T. (2005) Leaf internal diffusion conductance limits photosynthesis more strongly in older leaves of Mediterranean evergreen broad-leaved species. *Plant, Cell & Environment* **28**, 1552–1566.
- Niinemets U., Cescatti A., Rodeghiero M. & Tosens T. (2006) Complex adjustments of photosynthetic potentials and internal diffusion conductance to current and previous light availabilities and leaf age in Mediterranean evergreen species *Quercus ilex*. *Plant, Cell & Environment* **28**, 1552–1566.
- Oja V., Savchenko G., Jakob B. & Heber U. (1999) pH and buffer capacities of apoplastic and cytoplasmic cell compartments in leaves. *Planta* **209**, 239–249.
- Pfanz H. (1995) Apoplastic and symplastic proton concentrations and their significance for metabolism. In *Ecophysiology of Photosynthesis* (eds E.D. Schulze & M.M. Caldwell), pp. 103–122. Springer, Berlin Heidelberg, Germany and New York, NY, USA.
- Pinelli P. & Loreto F. (2003) (CO<sub>2</sub>)<sub>i</sub>-C<sup>12</sup> emission from different metabolic pathways measured in illuminated and darkened C<sub>3</sub> and C<sub>4</sub> leaves at low, atmospheric and elevated CO<sub>2</sub> concentration. *Journal of Experimental Botany* **54**, 1761–1769.
- Raschke K. (1979) Movement of stomata. In *Stable Isotopes. Integration of Biological, Ecological and Geochemical Processes* (eds W. Haupt & M.E. Feinleib), pp. 383–441. Springer, Berlin Heidelberg, Germany and New York, NY, USA.
- Ribas-Carbo M., Still C. & Berry J.A. (2002) Automated system for simultaneous analysis of δ<sup>13</sup>C, δ<sup>18</sup>O and CO<sub>2</sub> concentration in small air samples. *Rapid Communications in Mass Spectrometry* **16**, 339–345.
- Rogers A., Ellsworth D.S., Humphries S.W. (2001) Possible explanation of the disparity between *in vitro* and *in vivo* measurements of Rubisco activity: a study in loblolly pine at elevated pCO<sub>2</sub>. *Journal of Experimental Botany* **52**, 1555–1561.
- Sampol B., Bota J., Riera D., Medrano H. & Flexas J. (2003) Analysis of the virus-induced inhibition of photosynthesis in malmsey grapevines. *New Phytologist* **160**, 403–412.
- Savchenko G., Wiese C., Neimanis S., Hedrich R. & Heber U. (2000) pH regulation in apoplastic and cytoplasmic cell compartments of leaves. *Planta* **211**, 246–255.
- Schultz H.R. (1996) Leaf absorptance of visible radiation in *Vitis vinifera* L.: estimates of age and shade effects with a simple field method. *Scientia Horticulturae* **66**, 93–102.

- Sharkey T.D., Berry J.A. & Sage R.F. (1988) Regulation of photosynthetic electron-transport in *Phaseolus vulgaris* L., as determined by room-temperature chlorophyll a fluorescence. *Planta* **176**, 415–424.
- Sharkey T.D., Vassev T.L., Vanderveer P.J. & Vierstra R.D. (1991) Carbon metabolism enzymes and photosynthesis in transgenic tobacco (*Nicotiana tabacum* L.) having excess phytochrome. *Planta* **185**, 287–296.
- Siefritz F., Tyree M.T., Lovisolo C., Schubert A. & Kaldenhoff R. (2002) PIP1 plasma membrane aquaporins in tobacco: from cellular effects to function in plants. *Plant Cell* **14**, 869–876.
- Singsaas E.L., Ort D.R. & De Lucia E.H. (2004) Elevated CO<sub>2</sub> effects on mesophyll conductance and its consequences for interpreting photosynthetic physiology. *Plant, Cell & Environment* **27**, 41–50.
- Terashima I. & Ono K. (2002) Effects of HgCl<sub>2</sub> on CO<sub>2</sub> dependence of leaf photosynthesis: evidence indicating involvement of aquaporins in CO<sub>2</sub> diffusion across the plasma membrane. *Plant and Cell Physiology* **43**, 70–78.
- Tholen D., Boom C., Noguchi K. & Terashima I. (2007) The effects of chloroplast movement on CO<sub>2</sub> transfer conductance in *Arabidopsis thaliana*. *Plant and Cell Physiology* **48**, S95–S95.
- Tournaire-Roux C., Sutka M., Javot H., Gout E., Gerbeau P., Luu D.-T., Bligny R. & Maurel C. (2003) Cytosolic pH regulates root water transport during anoxic stress through gating of aquaporins. *Nature* **425**, 393–397.
- Uehlein N., Lovisolo C., Siefritz F. & Kaldenhoff R. (2003) The tobacco aquaporin NtAQP1 is a membrane CO<sub>2</sub> transporter with physiological functions. *Nature* **425**, 734–737.
- Valentini R., Epron D., De Angelis P., Matteucci G. & Dreyer E. (1995) In situ estimation of net CO<sub>2</sub> assimilation, photosynthetic electron flow and photorespiration in Turkey oak (*Quercus cerris* L.) leaves: diurnal cycles under different levels of water supply. *Plant, Cell & Environment* **18**, 631–640.
- Warren C.R. (2004) The photosynthetic limitation posed by internal conductance to CO<sub>2</sub> movement is increased by nutrient supply. *Journal of Experimental Botany* **55**, 2313–2321.
- Warren C.R. (2006) Estimating the internal conductance to CO<sub>2</sub> movement. *Functional Plant Biology* **33**, 431–442.
- Warren C.R. & Dreyer E. (2006) Temperature response of photosynthesis and internal conductance to CO<sub>2</sub>: results from two independent approaches. *Journal of Experimental Botany* **57**, 3057–3067.
- Xu L. & Baldocchi D.D. (2003) Seasonal trends in photosynthetic parameters and stomatal conductance of blue oak (*Quercus douglasii*) under prolonged summer drought and high temperature. *Tree Physiology* **23**, 865–877.
- Ye Q., Wiera B. & Steudle E. (2004) A cohesion/tension mechanism explains the gating of water channels (aquaporins) in *Chara* internodes by high concentration. *Journal of Experimental Botany* **55**, 449–461.
- Zeiger E., Talbott L.D., Frechilla S., Srivastava A. & Zhu J. (2002) The guard cell chloroplast: a perspective for the twenty-first century. *New Phytologist* **153**, 415–424.

Received 26 March 2007; received in revised form 8 June 2007; accepted for publication 11 June 2007